# Efficient Resonant Power Conversion

STANIMIR S. VALTCHEV AND J. BEN KLAASSENS

*Abstract*—**Power MOSFET's are still not powerful enough for thyristors, but for some applications, their features (such as the controllable turn-off capability) could present an advantage. The major losses in MOS devices are ohmic losses due to the on resistance of the device. The mode of operation and the precise region of improved efficiency are described for series-resonant power converters employing MOS transistors. This paper considers switching frequencies that are higher than the resonant frequency of the LC circuit only. The derived equations are generalized. Plots are used to discuss the selection of the switching frequency to maximize the efficiency.**

## I. Introduction

RESONANT conversion networks such as induction heating appliances of low and medium power levels are implemented by power transistors. During experiments with resonant loads, variation in the efficiency of energy transfer is observed, depending on the frequency of excitation with respect to the resonant frequency of the load. Because of the significant variation in the resonant frequency of the load in these technological processes and the ease of operation at different frequencies with power transistors (including MOSFET's), the appropriate frequency range for an efficient performance is suggested.

Numerous papers have been written on the subject of operating radio transmitters more efficiently by out-tuning from the resonant frequency of the output LC tank connected to the antenna. This mode of operation was considered by Natchev for power converters for inductive heating [1]. Of course, those solutions were implemented by electronic vacuum tubes because thyratrons and other latchable devices could not operate at frequencies higher than or even close to the resonant frequency of the process. It has been mentioned in more recent publications [2]–[6] that resonant loads operating at frequencies higher than the resonant frequency will make the operation both more efficient and safer. The explanation has its roots in the physics of modern semiconductor devices but how much the switching frequency should be increased or the reason why was not understood.

The objective is to present the analysis of the series-resonant converter, especially those operating above resonant frequency using power FET switches. The results are used to analyze the current form factor and its effect on the efficiency both experimentally and theoretically. The selection of frequencies lower than the resonant frequency is also taken into account.

Manuscript received July 24, 1989; revised June 7, 1990.

S. S. Valtchev was with the Laboratory for Power Electronics, Delft University of Technology Delft, the Netherlands. He is now with the Higher Institute for Mechanical and Electrical Engineering "VMEI Lenin," Sofia, Bulgaria.

J. B. Klaassens is with the Laboratory for Power Electronics, Delft University of Technology, Delft, the Netherlands.

IEEE Log Number 9040019.

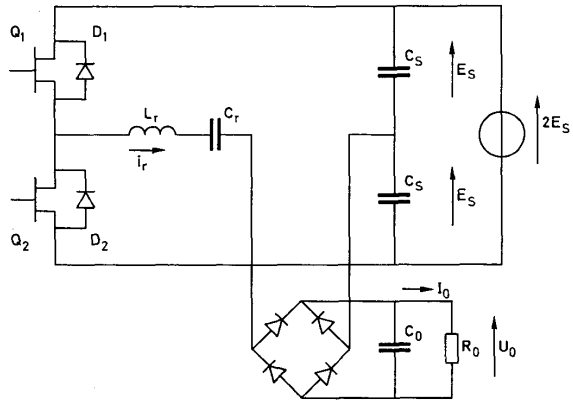


Fig. 1. Schematic diagram of the transistorized resonant converter.

## II. Principles of Operation

A simplified schematic of the power circuit of the resonant converter is shown in Fig. 1. Its mode of operation consists of the alternate closing of the semiconductor switches $Q1$ and $Q2$ and the associated antiparallel diodes $D1$ and $D2$. The load is in series with the series-resonant circuit. An alternating resonant current $i_r$ is generated in the series-resonant circuit with passive components $L_r$ and $C_r$. The average value of the load current $I_o$ is related to this resonant current by $I_o = |i_r|_{av}$.

The circuit may be operated at pulse frequencies above or below resonant frequency $f_r$ of the resonant circuit, as discussed in [6]. A main advantage of operating above a resonant frequency for the converter is that there are no diode or FET switching losses. The turn-on losses in the FET switch are negligible because its inverse diode carries current, and the voltage over the switch is zero before the FET goes into conduction. There are also no switching stresses applied to the diode. The diode can be of medium speed. However, to achieve those advantages, the semiconductor switch must turn off current and is therefore subjected to turn-off switching losses. Lossless snubbers can easily be applied to the FET devices.

Operation below the resonant frequency results in turn-on switching losses and diode switching losses. High-speed diodes are necessary. Another disadvantage will be the design of the input and output filters, which must be laid out for the minimum switching frequency. FET turn-off occurs in a lossless way when operating below resonant frequency, but the turn on is started with a short-circuit connection through the diode of the opposite switch.

Therefore, operation of the resonant converter above resonance seems to be the proper choice for many power supplies operating at high frequencies. This paper analyzes the con-

0278-0046/90/1200-0490$01.00 

duction losses of the switches in a series-resonant series-loaded converter operating below and above resonant frequency.

## III. Efficiency

To indicate the difference in efficiency $\eta$ between the operation at specific values for the pulse frequency, the ohmic losses that are rooted in the resistive elements of the end-stage are presented as $P_{\text{loss}}$. The end stage may be composed of power switching devices, rectifiers, magnetic and capacitive components, and wiring. The resistor $R_{\text{loss}}$ represents the total ohmic losses in the converter network. The power $P_o$ is supplied to the output with a voltage $U_o$ and a current $I_o$. The reciprocal of the efficiency $\eta$ is expressed by

$$\eta^{-1} = (P_o + P_{\text{loss}})/P_o \tag{1}$$

where

$$P_{\text{loss}} = I_{rms}^2 R_{\text{loss}} \tag{2}$$

$$P_o = U_o I_o = (I_o R_o) I_o \tag{3}$$

where $I_{rms}$ is the rms value of the resonant current $i_r$ flowing through the resonant network. Since the average value of the output current $I_o$ is identical to the average value of the rectified resonant current $|i_r|$ (see Fig. 1), i.e.

$$I_o = \frac{1}{T_p}\int_0^{T_p} |i_r|\, dt \tag{4}$$

expression (1) is rewritten as

$$\eta^{-1} = 1 + \frac{I_{rms}^2}{I_o^2}\frac{R_{\text{loss}}}{R_o} = 1 + \frac{R_{\text{loss}}}{R_o}\rho_i^2 \tag{5}$$

which gives a useful relation between the efficiency $\eta$ and the shape of the resonant current expressed by the current form factor

$$\rho_i = I_{rms}/I_o \tag{6}$$

which may deviate depending on the mode of operation. Approaching the square wave shape with the minimal value for the current form factor $\rho_i$ equal to one is not possible in a series-resonant circuit. It is advisable to operate with continuous waveforms and to minimize the resistances of the circuit including switches and rectifiers. The dynamic losses that occur during the switching process will be briefly discussed later. To minimize the on-resistance $R_{DS(\text{on})}$ of the power FET switches, continuous waveforms are advantageous because the resistance $R_{DS(\text{on})}$ increases along with increasing drain current [9].

## IV. Current Form Factor

The relations between the current form factor $\rho_i$, the average output current $I_o$, the pulse repetition frequency $f_p$, etc. are well defined in [7] in regard to pulse repetition frequencies lower than the resonant frequency. For higher frequencies, the analysis of the internal waveforms of the resonant converter has to be performed.

Fig. 2 shows the generated waveforms for the resonant current $i_r$ and the resonant capacitor voltage $u_{Cr}$, where the pulse length $x_0 = \psi_1 + \psi_2$ is equal to the half period of the switching frequency $f_p$. The voltage $U_{LC}$ is the *excitation voltage* energizing the LC circuit. This voltage is considered to be constant throughout every particular time interval of the resonant current pulse.

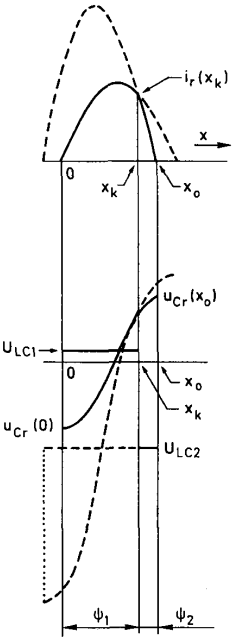

Fig. 2. Characteristic waveforms.

The initial conditions are

$$i_r(0) = 0 \tag{7}$$

$$u_{Cr}(0) \neq 0. \tag{8}$$

For the cyclic-stable mode of operation, a boundary value problem is denoted as

$$i_r(x_0) = i_r(0) = 0 \tag{9}$$

$$u_{Cr}(x_0) = -u_{Cr}(0) \neq 0. \tag{10}$$

The process of switching is repeated with an alternating polarity for every switching half period.

Introduce normalized voltages and currents (superscript $N$):

| | |
|---|---|
| $u_{Cr}^N(x) = u_{Cr}(t)/E_s$ | normalized capacitor voltage |
| $U_{LC}^N = U_{LC}/E_s$ | normalized excitation voltage |
| $Z_r i_r^N(x) = Z_r i_r(t)/E_s$ | normalized current |
| $x = \omega_r t$ | normalized time |

where

| | |
|---|---|
| $\omega_r = 2\pi f_r = 1/\sqrt{L_r C_r}$ | resonant frequency |
| $Z_r = \sqrt{L_r/C_r}$ | characteristic impedance. |

The state equation of the resonant circuit is written as

$$\frac{d}{dx}\begin{bmatrix} Z_r i_r^N(x) \\ u_{Cr}^N(x) \end{bmatrix} = \begin{bmatrix} 0 & -1 \\ 1 & 0 \end{bmatrix}\begin{bmatrix} Z_r i_r^N(x) \\ u_{Cr}^N(x) \end{bmatrix} + \begin{bmatrix} U_{LC}^N \\ 0 \end{bmatrix}. \tag{11}$$

The general solution of this equation is

$$u_{Cr}^N(x) = U_{LC}^N - \left[U_{LC}^N - u_{Cr}^N(0)\right]\cos(x) + Z_r i_r^N(0)\sin(x) \quad (12)$$

$$Z_r i_r^N(x) = \left[U_{LC}^N - u_{Cr}^N(0)\right]\sin(x) + Z_r i_r^N(0)\cos(x). \quad (13)$$

### A. Time Interval $[0, x_k]$

A resonant current pulse is composed of two sinusoidal current segments with individual time length $\psi_1 = x_k$ and $\psi_2 = x_0 - x_k$, as shown in Fig. 2. The first segment of the resonant current pulse is initiated at the time $x = 0$ by applying an excitation voltage $U_{LC1}$ to the resonant network. When transistor $Q1$ or $Q2$ is turned on (see Figs. 1 and 2), the excitation voltage $U_{LC1}^N$ is a combination of the voltages of the source and load. For a positive resonant current pulse, the excitation voltage is written as

$$U_{LC1}^N = 1 - q > 0 \quad (14)$$

where $q$ is the normalized output voltage defined as the conversion ratio $q = U_o/E_s$. This segment is described by the general solution (12) and (13)

$$u_{Cr}^N(x) = U_{LC1}^N - \left[U_{LC1}^N - u_{Cr}^N(0)\right]\cos(x) \quad (15)$$

$$Z_r i_r^N(x) = \left[U_{LC1}^N - u_{Cr}^N(0)\right]\sin(x). \quad (16)$$

The end point $x = x_k$ of the first segment of the resonant waveforms is expressed by

$$u_{Cr}^N(x_k) = U_{LC1}^N - \left[U_{LC1}^N - u_{Cr}^N(0)\right]\cos(x_k) \quad (17)$$

$$Z_r i_r^N(x_k) = \left[U_{LC1}^N - u_{Cr}^N(0)\right]\sin(x_k). \quad (18)$$

### B. Time Interval $[x_k, x_0]$

The *second segment* of the resonant current pulse is initiated at the time $x = x_k$ by applying the excitation voltage $U_{LC2}$ to the resonant network. This corresponds to switching off transistor $Q1$ or $Q2$ (see Figs. 1 and 2). The current is now supported by the antiparallel diode against the voltages $E_s$ and $U_o$ resulting in an excitation voltage

$$U_{LC2}^N = -1 - q < 0. \quad (19)$$

This segment is also described by the general solution (12) and (13).

### C. Cyclic-Stable Condition

Taking into account that the conversion process is in the steady state, we can calculate the second part of the half period, applying the boundary values of (9) and (10).

From the expressions (9), (10), (12), (13), (17), and (18), we can assemble the values of the resonant current and resonant capacitor voltage in equations, representing the end values for the time interval $[x_k, x_0]$

$$u_{Cr}^N(x_0) = U_{LC2}^N - \left[U_{LC2}^N - U_{LC1}^N + \left\{U_{LC1}^N - u_{Cr}^N(0)\right\}\cos(x_k)\right]\cos(x_0 - x_k) + \left[U_{LC1}^N - u_{Cr}^N(0)\right]\sin(x_k)\sin(x_0 - x_k) = -u_{Cr}^N(0) \quad (20)$$

$$Z_r i_r^N(x_0) = \left[U_{LC2}^N - U_{LC1}^N + \left\{U_{LC1}^N - u_{Cr}^N(0)\right\}\cos(x_k)\right]\cdot\sin(x_0 - x_k) + \left[U_{LC1}^N - u_{Cr}^N(0)\right]\cdot\sin(x_k)\cos(x_0 - x_k) = 0. \quad (21)$$

In the switching circuit of Fig. 1, the excitation voltages $U_{LC1}^N$ and $U_{LC2}^N$ are different in order to transfer energy and to stabilize the internal waveforms. In addition, $U_{LC1}^N \neq u_{Cr}^N(0)$ and $U_{LC2}^N \neq -u_{Cr}^N(0)$; otherwise, we would not obtain any oscillation at all.

To obtain expressions for the length of each time interval $\psi_1 = x_k$ and $\psi_2 = x_0 - x_k$, we can transform (20) and (21) into

$$\cos(x_0 - x_k) = \frac{U_{LC2}^N - U_{LC1}^N + \left[U_{LC1}^N - u_{Cr}^N(0)\right]\cos(x_k)}{u_{Cr}^N(0) + U_{LC2}^N} \quad (22)$$

$$\sin(x_0 - x_k) = \frac{\left[u_{Cr}^N(0) - U_{LC1}^N\right]\sin(x_k)}{u_{Cr}^N(0) + U_{LC2}^N}. \quad (23)$$

The initial values of the waveforms for the second segment are easily derived from (22) and (23) with (10), (17), and (18):

$$u_{Cr}^N(x_k) = U_{LC2}^N - \left[U_{LC2}^N - u_{Cr}^N(x_0)\right]\cos(x_k - x_0) \quad (24)$$

$$Z_r i_r^N(x_k) = \left[U_{LC2}^N - u_{Cr}^N(x_0)\right]\sin(x_k - x_0). \quad (25)$$

Equations (24) and (25) describing the second segment are similar to (17) and (18), which describe the first resonant segment for steady-state conditions.

We can generalize (24) and (25) for the second part of the half period of switching in a way similar to (15) and (16) as

$$u_{Cr}^N(x) = U_{LC2}^N - \left[U_{LC2}^N - u_{Cr}^N(x_0)\right]\cos(x - x_0) \quad (26)$$

$$Z_r i_r^N(x) = \left[U_{LC2}^N - u_{Cr}^N(x_0)\right]\sin(x - x_0). \quad (27)$$

For both time intervals $[0, x_k]$ and $[x_k, x_0]$, the resonant current and the resonant capacitor voltage are sinusoidal waveforms, as shown in Fig. 2. Both time intervals are linked at the time $x = x_k$.

Since the expressions are normalized, we can apply them to the analysis of the operation at frequencies lower and higher than the resonant frequency for step-down ($q > 0$) or step-up ($q < 0$) converters and for transistors as well as for thyristors. We can now calculate all the necessary values for the current form factor $\rho_i$ to evaluate its effect on the efficiency.

### D. Energy Balance

For the cyclic-stable mode of operation, the energy delivered to the LC tank is equal to the energy withdrawn from it because no energy is consumed inside the LC circuit:

$$W_{LC} = \int_0^{x_k} U_{LC1} i_r \, dx + \int_{x_k}^{x_0} U_{LC2} i_r \, dx = 0. \quad (28)$$

Substituting the expressions for the resonant current (16) and (27) for each part of the half period into (28) for $Z_r \neq 0$, we

can transform (28) into

$$U^N_{LC1}\left[U^N_{LC1} - u^N_{Cr}(0)\right]\left[1 - \cos(x_k)\right] = U^N_{LC2}\left[U^N_{LC2} + u^N_{Cr}(0)\right]\left[1 - \cos(x_k - x_0)\right]. \quad (29)$$

Comparing $u_{Cr}(x_k)$ to both (24) and (17) gives a third equation, which, combined with (29), is solved for the angles

$$\cos(x_k) = \frac{U^N_{LC2}\left[U^N_{LC1} + u^N_{Cr}(0)\right] + U^N_{LC1}\left[u^N_{Cr}(0) - U^N_{LC1}\right]}{\left[U^N_{LC1} - U^N_{LC2}\right]\left[u^N_{Cr}(0) - U^N_{LC1}\right]} \quad (30)$$

$$\cos(x_0 - x_k) = \frac{U^N_{LC1}\left[U^N_{LC2} - u^N_{Cr}(0)\right] - U^N_{LC2}\left[u^N_{Cr}(0) + U^N_{LC2}\right]}{\left[U^N_{LC1} - U^N_{LC2}\right]\left[u^N_{Cr}(0) + U^N_{LC1}\right]}. \quad (31)$$

If we substitute

$$\theta_1 = \frac{U^N_{LC1} + u^N_{Cr}(0)}{U^N_{LC1} - u^N_{Cr}(0)} \quad (32)$$

$$\theta_2 = \frac{U^N_{LC2} - u^N_{Cr}(0)}{U^N_{LC2} + u^N_{Cr}(0)} \quad (33)$$

the expressions (30) and (31) become more compact

$$\cos(x_k) = \frac{U^N_{LC1} - \theta_1 U^N_{LC2}}{U^N_{LC1} - U^N_{LC2}} \quad (34)$$

$$\cos(x_0 - x_k) = \frac{U^N_{LC2} - \theta_1 U^N_{LC1}}{U^N_{LC2} - U^N_{LC1}}. \quad (35)$$

These equations summarize all possible modes of operation and can be applied at switching frequencies both lower and higher than the resonant frequency. The equations can also be applied for a resonant converter operating with a reversed power flow, assuming there are controlled rectifiers connected to the load.

The analysis is now applied to the operation at frequencies higher than the resonant frequency because for lower frequencies, the expressions are identical to those in [7].

The resonant capacitor voltage $u_{Cr}$ reaches an extreme at moments $x = 0$ and $x = x_0$ when its first derivative (i.e., the resonant current) crosses zero. For the cyclically stable mode of operation, $u_{Cr\max}$ is equal either to $-u_{Cr}(0)$ or $u_{Cr}(x_0)$. The variation of the voltage over the resonant capacitor $2u_{Cr\max}$ is hence the average value of the resonant current $Z_r i_r$ over the half period $[0, x_0]$; therefore

$$Z_r I^N_o = 2u^N_{Cr\max}/x_0. \quad (36)$$

If we introduce a more compact notation of phase angles $\psi_1$ and $\psi_2$ of the time intervals of the resonant current as shown in Fig. 2 (in the practical case of $2\pi f_p > \omega_r$)

$$\psi_1 = x_k = \arccos\left(\frac{1 - q - qu^N_{Cr\max}}{1 - q + u^N_{Cr\max}}\right) \quad (37)$$

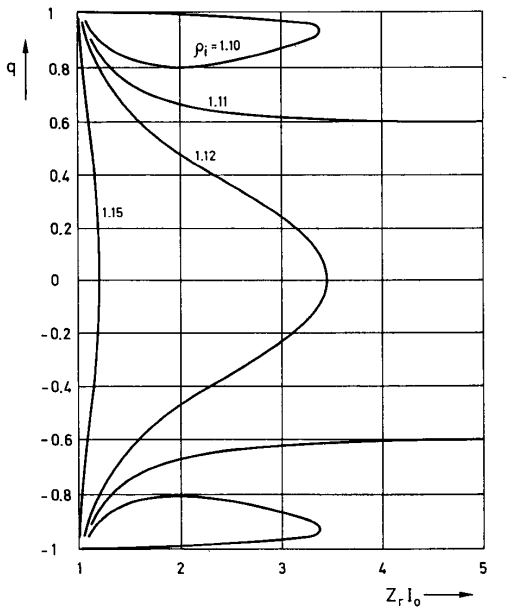


Fig. 3. Normalized output characteristic for a constant value of the current form factor $\rho_i$.

$$\psi_2 = (x_0 - x_k) = \arccos\left(\frac{1 + q + qu^N_{Cr\max}}{1 + q + u^N_{Cr\max}}\right). \quad (38)$$

The rms value of the continuous resonant current is calculated from

$$\left(Z_r I^N_{rms}\right)^2 = \left\{\left(Z_r i^N_{f\max}\right)^2\left[\psi_1 - \tfrac{1}{2}\sin(2\psi_1)\right] + \left(Z_r i^N_{r\max}\right)^2\left[\psi_2 - \tfrac{1}{2}\sin(2\psi_2)\right]\right\}/(2x_0) \quad (39)$$

where $Z_r i^N_{f\max}$ and $Z_r i^N_{r\max}$ are the normalized amplitudes (virtual amplitude when the amplitude is not visible in the time interval $\psi_1$ or $\psi_2$) of the resonant current segments, as in (16) and (27), with practical values in our case

$$Z_r i^N_{f\max} = \left[U^N_{LC1} - u^N_{Cr}(0)\right] = 1 - q + u^N_{Cr\max} \quad (40)$$

$$Z_r i^N_{r\max} = \left[U^N_{LC2} - u^N_{Cr}(0)\right] = -1 - q - u^N_{Cr\max}. \quad (41)$$

## V. Computer Analysis

The value of the current form factor $\rho_i$ is obtained by dividing the rms current $I^N_{rms}$ (39) by the average current $I^N_o$ (36). Computer calculations were used to produce the normalized output characteristics as the relation between the conversation ratio $q$ and the average value of the normalized output current $Z_r I_o$, as shown in Fig. 3.

It was established theoretically that the current form factor $\rho_i$ is less than $2/\sqrt{3} = 1.155$, which is better than some modes of continuous current at frequencies lower than the resonant frequency [7].

Fig. 3 shows that the optimal area of operation for this class of converters should be for higher values of the conversion ratios $q$. For $q \geq 0.5$, the current form factor could be

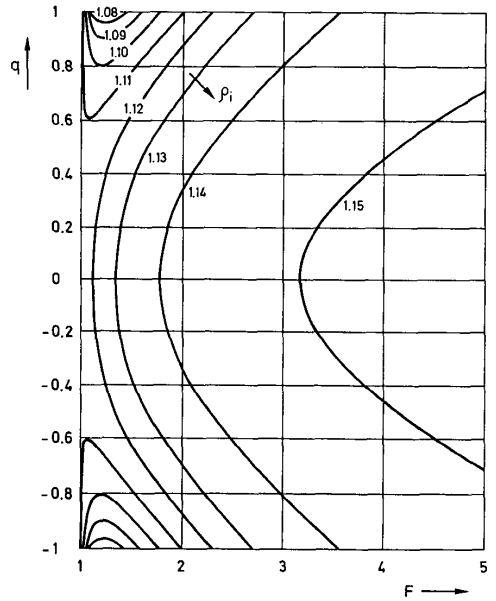


Fig. 4. Conversation ratio $q$ as a function of frequency ratio $F = f_p/f_{res}$ for a constant value of the current form factor $\rho_i$.

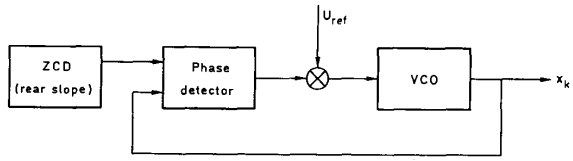


Fig. 5. Experimental control circuitry

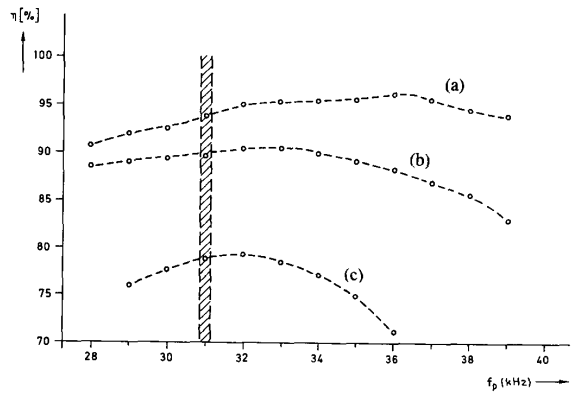


Fig. 6. Efficiency $\eta$ of the power conversion process related to the switching frequency: (a) Lower power, high $q$; (b) low power, low $q$; (c) high power, high $q$.

better than the one of the $\rho_i = \pi/2\sqrt{2} = 1.1107$). The region of an effective operation is expanded especially at higher currents (close to but higher than the resonant frequency).

To understand how the switching frequency $f_p$ influences the current form factor, the relation between the conversion ratio $q$ and the relative frequency $F = f_p/f_{res}$ is shown in Fig. 4 for $F > 1$ as well as for a constant value of the current form factor $\rho_i$. The current form factor shows limited variations for a constant switching frequency that is greater than the resonant frequency.

We can say that up $F = 2$ (and especially with $q$ tending to higher values), the efficiency is better than at resonance. It can be shown that it is not possible to reach $q = 1$ ($U_{LC1} = U_{LC2}$, which implies no oscillations at all), as is indicated in both Figs. 3 and 4.

To conclude, it could be said that looking at Fig. 4 for every value of the conversion ratio $q$, a particular frequency could be found with a minimal current form factor (thus maximal efficiency). This selected frequency may lead to efficiencies that are even better than those at the resonant frequency if the output voltage is at least greater than half the supply voltage ($q > 0.5$).

## VI. Experimental Work

An electronic circuit shown in Fig. 5 was designed and constructed to ensure a phase shift between the rear slope of the resonant current at the zero-crossing point and the rear slope of the control gate-drive pulse. In practice, the control of the output voltage for a dc-dc converter is realized with pulse frequency modulation.

Experiments were carried out on a 1-kW half-bridge converter in combination with a full-bridge rectifier, as was already shown in Fig. 1. The rectifier bridge is connected to the load, which consists of a resistor in parallel with a filter capacitor. The converter applies power MOSFET's, which are capable of current turn-off as required for switching frequencies higher than the resonant frequency. The losses of these devices entirely depends on the on resistance.

Parallel loading of the resonant capacitor was also experimentally verified, but the efficiency of this mode of operation is subject to different considerations with respect to the indicated idealizations and has been investigated in Steigerwald's work [6].

In Fig. 6, the efficiency for a different series loading is plotted as a function of the switching frequency. The shaded area indicates the resonant frequency of the $LC$ circuit. In this figure, a shift of the maximum efficiency is clearly observable for different loading. This shift, and the occurrence of a maximum efficiency at frequencies higher than the resonant frequency, demonstrates the importance of the ohmic conduction losses to the total efficiency. This corresponds with the results of the analysis of the areas of efficient energy conversion with series-resonant converters. If there were no losses other than dynamic losses, the efficiency would decrease along with the frequency.

In order to understand the entire process including the switching phenomena, the shape of the characteristic current and voltage waveforms were recorded and analyzed in the experimental converter. In Figs. 7 and 8, the resonant current $i_r$ and the current through the switches are shown for a switching frequency that is both lower and higher than the resonant frequency.

It is well known that because of the recovery time of the freewheeling diodes, a short circuit is introduced at the moment a transistor is turned "on" for frequencies lower

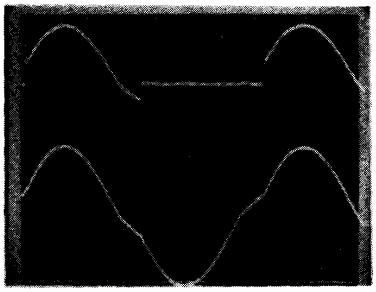

Fig. 7. Waveforms for switching frequency lower than the resonant frequency (timescale: 5 $\mu$/div. Upper trace: current through the switch $i_{sw}$ (30 A/div); lower trace: resonant current $i_r$ (25 A/div).

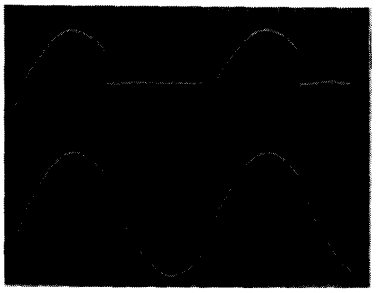

Fig. 8. Waveforms for a switching frequency higher than the resonant frequency (timescale: 5 $\mu$s/div). Upper trace: current through the switch $i_{sw}$ (30 A/div); lower trace: resonant current $i_r$ (25 A/div).

than the resonant frequency, as can be seen from Fig. 7. The input capacitance of the power MOSFET's (including the Miller effect) slows down and delays the rise of the gate voltage. Since the on resistance $R_{DS(on)}$ of a power MOSFET is strongly dependent on the gate voltage, the losses increase [8], [9].

For operation above the resonant frequency, this problem is eliminated since the switches are turned on at zero current, as is shown in Fig. 8 (the transistor is allowed to conduct while its antiparallel diode is still conducting). The slow rising of the gate voltage will not influence the efficiency at higher conversion frequencies.

For frequencies that are lower than the resonant frequency, a large leap of dissipation is caused when the transistor is turned on and for higher frequencies when the transistor is turned off.

Switching at higher frequencies has the advantage that for the continuous mode of operation, the transistor is switched "on" when zero or almost zero voltage is applied to it. This makes it possible to apply nondissipative snubbers to reduce the turn-off losses, as is well known from [2]. The experiments with capacitive snubbers revealed a decrease of the losses, which were measured directly at the switching transistor by approximately 2 to 4%.

## VII. Conclusions

The dc analysis of the series-resonant converter is presented operating above resonant frequency, which is used to analyze the current form factor and its effect on the efficiency both experimentally and theoretically. Plots are used to discuss the selection of the switching frequency in order to maximize the efficiency.

The derived expressions are generalized and can be applied to calculations in any of the switching modes for a series-resonant circuit. For switching frequencies higher than the resonant frequency, an area of more efficient operation is indicated, which will aid in the design of this class of converters and power supplies. It is pointed out that (especially for the power MOSFET's where the ohmic losses dominate) it is more attractive to select switching frequencies that are higher than the resonant frequency because of the possibility of nondissipative snubbers. Slowing down the rise of the gate voltage and, hence, the slow decrease of "on" resistance during turn on is also not a drawback to high-frequency switching. Because of this safer operation, the standard intrinsic diode of the power MOSFET could be used at high frequencies instead of the more expensive FREDFET.

## References

[1] N. Natchev, Doctoral thesis, VME Institute, Faculty Transport Commun., Sofia, 1960 (in Bulgarian).

[2] R. Steigerwald, "High frequency resonant transistor, DC-DC," *IEEE Trans. Ind. Electron.*, vol. IE-31, no. 2, pp. 181-191, 1984.

[3] A. F. Witulski and R. W. Erickson, "Steady-state analysis of the series resonant converter," *IEEE Trans. Aerospace Electron. Syst.*, vol. AES-21, no. 6, pp. 791-799, 1985.

[4] —, "Design of the series resonant converter for minimum component stress," *IEEE Trans. Aerospace Electron. Syst.*, vol. AES-22, no. 4, pp. 356-363, 1986.

[5] J. Ferrieux, J. Lavieville, and J. Perard, "Analysis and modeling of DC-DC resonant converter: Application of the resonant switch-mode power supply," in *Proc. IEE Conf. Power Electron. Variable Speed Drives* (Birmingham, England), 1986, pp. 158-163.

[6] R. Steigerwald, "A comparison of half-bridge resonant converter topologies," in *Proc. IEEE Appl. Power Electron. Conf.* (San Diego, CA), 1987, pp. 135-144.

[7] J. B. Klaassens, "Steady-state analysis of a series-resonant DC-DC converter with a bipolar power flow," *IEEE Trans. Ind. Electron.*, vol. 36, no. 1, pp. 48-55, 1989.

[8] B. R. Pelly, "Power MOSFET's—A status review," in *Proc. IEEJ Int. Power Electron. Conf.* (Tokyo, Japan), 1983, pp. 19-32.

[9] C. Kirkman and M. J. Turner, "On-resistance performance of MOSFET's," in *Proc. PCI Conf.*, Sept. 1982, pp. 99-110.